BIOCHEMISTRY
including biophysical chemistry & molecular biology

Article

pubs.acs.org/biochemistry

Mapping the tRNA Binding Site on the Surface of Human DNMT2 Methyltransferase

Tomasz P. Jurkowski,[†] Raghuvaran Shanmugam,[†] Mark Helm,[‡] and Albert Jeltsch*,[†]

[†]Biochemistry Laboratory, School of Engineering and Science, Jacobs University Bremen, Campus Ring 1, 28759 Bremen, Germany, and Institute of Biochemistry, Faculty of Chemistry, Stuttgart University, Pfaffenwaldring 55, 70569 Stuttgart, Germany

[‡]Institute of Pharmacy and Biochemistry, Johannes Gutenberg-Universität Mainz, Staudinger Weg 5, 55128 Mainz, Germany

Supporting Information

ABSTRACT: The DNMT2 enzyme methylates tRNA-Asp at position C38. Because there is no tRNA−Dnmt2 cocrystal structure available, we have mapped the tRNA binding site of DNMT2 by systematically mutating surface-exposed lysine and arginine residues to alanine and studying the tRNA methylation activity and binding of the corresponding variants. After mutating 20 lysine and arginine residues, we identified eight of them that caused large (>4-fold) decreases in catalytic activity. These residues cluster within and next to a surface cleft in the protein, which is large enough to accommodate the tRNA anticodon loop and stem. This cleft is located next to the binding pocket for the cofactor *S*-adenosyl-L-methionine, and the catalytic residues of DNMT2 are positioned at its walls or bottom. Many of the variants with strongly reduced catalytic activity showed only a weak loss of tRNA binding or even bound better to tRNA than wild-type DNMT2, which suggests that the enzyme induces some conformational changes in the tRNA in the transition state of the methyl group transfer reaction. Manual placement of tRNA into the structure suggests that DNMT2 mainly interacts with the anticodon stem and loop.

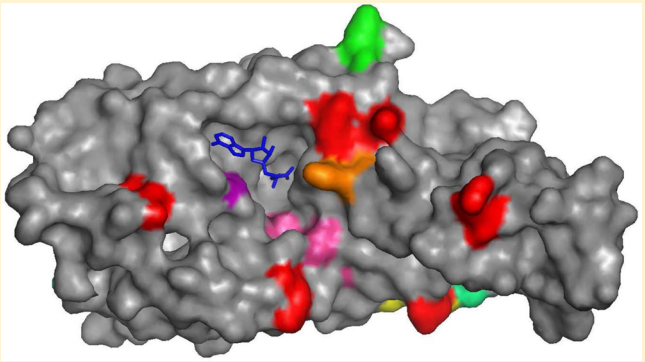

The Dnmt2 enzyme was originally assigned as a member of the DNA methyltransferase family on the basis of its very high degree of similarity in sequence and structure to eukaryotic and prokaryotic DNA-(cytosine C5)-methyltransferases.[1−4] Dnmt2 is strongly conserved and can be found in species ranging from *Schizosaccharomyces pombe* to humans, suggesting a very important role in cellular homeostasis.[4,5] However, DNA methylation activity of DNMT2 was undetectable or very weak.[3,6−12] Moreover, most *dnmt2* knockout organisms originally lacked an apparent phenotype[6,10] such that Dnmt2's biological function remained unknown. In a seminal paper, Goll and colleagues discovered that Dnmt2 is an active RNA methyltransferase capable of methylating position C38 of the $tRNA^{Asp}$ from mouse, *Arabidopsis thaliana*, and *Drosophila melanogaster*.[10] Later, a robust tRNA methylation activity of Dnmt2 was also confirmed by others.[13−16]

We have shown that DNMT2 methylates RNA by employing a DNA methyltransferase-like catalytic mechanism, which is clearly different from the mechanism of other RNA MTases.[13] DNA-(cytosine C5)-methyltransferases employ three key catalytic elements that are located in amino acid sequence motifs conserved within this family of enzymes.[17,18] DNA methylation is initiated by a nucleophilic attack of a catalytic cysteine residue located in the conserved amino acids sequence motif IV at position C6 of the target cytosine. This is supported by a conserved glutamate residue from motif VI and two arginine residues from motif VIII.[18] In DNMT2, the corresponding residues are C79, E119, R160, and R162. Exchange of these residues with alanine led to variants with no detectable in vitro tRNA methylation activity.[13] This unique DNA MTase-like reaction mechanism of RNA methylation suggested that this enzyme changed its substrate specificity from DNA to RNA in the course of its evolution. This hypothesis was supported by phylogenetic evidence based on a detailed analysis of more than 5000 prokaryotic and eukaryotic m5C DNA methyltransferases.[5]

Goll and colleagues have identified the human $tRNA^{Asp}$ as the methylation target of human DNMT2,[10] but later *Drosophila* $tRNA^{Gly(GCC)}$ and $tRNA^{Val(AAC)}$ [15] as well as $tRNA^{Glu(UUC)}$ from *Dictyostelium discoideum* (Mueller et al., manuscript submitted for publication) were also shown to be Dnmt2 substrates. However, neither the tRNA specificity determinants nor the tRNA binding pocket in the Dnmt2 enzyme is known. Because there is no tRNA−Dnmt2 cocrystal structure available, we have mapped the tRNA binding site of DNMT2 by systematically mutating several conserved surface-exposed lysine and arginine residues and studying the tRNA

Received: February 27, 2012
Revised: May 14, 2012
Published: May 16, 2012

dx.doi.org/10.1021/bi3002659 | *Biochemistry* 2012, 51, 4438−4444

methylation activity and binding of the variants. The rationale behind this approach was that nucleic acid binding pockets in proteins usually contain lysine and arginine residues that are engaged in electrostatic interactions with the phosphodiester backbone. Indeed, we could identify one clearly defined DNMT2 surface region that is involved in $tRNA^{Asp}$ interaction. It forms a cleft that is sufficiently large to accommodate parts of the tRNA and is next to the binding pocket of the cofactor *S*-adenosyl-L-methionine (AdoMet). The catalytic residues of DNMT2 are located at the bottom and in the walls of the tRNA binding cleft.

EXPERIMENTAL PROCEDURES

Plasmids, Oligonucleotides, and Site-Directed Mutagenesis. The construction of the pET28a plasmid encoding the human DNMT2 wild-type and C79A mutant proteins (both in fusion with an N-terminal His_6 tag) has been described previously.[7,13] The variants of human DNMT2 were created by the megaprimer site-directed mutagenesis method as described previously.[19] All generated constructs were sequenced to check for the absence of undesired additional mutations.

Structural Modeling of DNMT2. The crystal structure of human DNMT2 is missing residues 79−96 and 189−247, which are localized in apparently mobile loops.[3] Because some of the residues that we investigated are placed in these loops, we have added the loops using homology modeling with Modeler.[20] For this, the DNMT2 protein sequence was aligned with the sequence from the DNMT2 crystal structure and submitted for homology modeling using Modeler (with five levels of model refinement). Ten homology models were obtained; the model with the arbitrarily most realistic (most compact) structure was chosen. SAH was added to the model after superposition with the original crystal structure in DeepView.[21] It has to be noted that the introduced loops are only very roughly positioned and should be used only as a guide for discussion.

Protein Expression and Purification. The human His_6-tagged DNMT2 fusion proteins were expressed in *Escherichia coli* (DE3) Rosetta2 pLysS (Novagen) cells at 37 °C in LB medium containing kanamycin (25 μg/mL). The cells were induced at an OD_{600} of 0.6 with 1 mM IPTG and harvested 3 h after induction. The protein purification was performed as described previously.[13] Protein concentrations were determined by UV spectroscopy using a molar extinction coefficient for His_6-DNMT2 (ε) of 19920 M^{-1} cm^{-1}.

In Vitro Transcription of tRNA and Radioactive Labeling. The DNA template encoding *D. melanogaster* $tRNA^{Asp}$ preceded by the T7 promoter (tRNAAsp_Dm_wt_templ, 5′-TAA TAC GAC TCA CTA TAG GCC TCG ATA GTA TAG TGG TTA GTA TCC CCG CCT GTC ACG CGG GAG ACC GGG GTT CAA TTC CCC GTC GGG GCG CCA-3′) was amplified in a standard polymerase chain reaction (PCR) using T7 primer (5′-CGC GCG AAG CTT AAT ACG ACT CAC TAT A-3′) and $tRNA^{Asp}$ primer (5′-TGG CGC CCC GAC GGG GAA TTG-3′). For in vitro transcription, 100 μL of the PCR mixture was incubated with 200 μL of 2× transcription buffer [80 mM Tris-HCl (pH 8.1), 2 mM spermidine, 10 mM DTT, 0.02% Triton X-100, 60 mM $MgCl_2$, and 4 μg/mL BSA], NTPs (200 μM each), and 5−10 μL of T7 polymerase (Fermentas) in a total volume of 400 μL for 3 h at 37 °C. Transcripts were purified over 12% denaturing polyacrylamide gel electrophoresis (PAGE); RNA was visualized by UV shadow casting, and the appropriate bands were excised, eluted in buffer containing 50 mM Tris-HCl (pH 7.5), 300 mM sodium acetate, and 0.5% sodium dodecyl sulfate (SDS) at room temperature overnight, and precipitated with 2.5 volumes of 100% ethanol at −20 °C. After centrifugation, pellets were washed once with 80% ice-cold ethanol, dried, and subsequently dissolved in water. Radioactively labeled *D. melanogaster* $tRNA^{Asp}$ was prepared by in vitro transcription following a protocol similar to that for unlabeled tRNA; however, the standard reaction mixture was supplemented with 0.3125 μM [α-^{32}P]ATP (Hartmann Analytic, Braunschweig, Germany), and the concentration of ATP was decreased to 25 μM in a total reaction volume of 100 μL.

Circular Dichroism. To confirm that the introduced mutations do not alter the proper folding of the mutant proteins, we have measured the far-UV circular dichroism spectra on a Jasco J-815 circular dichroism spectrophotometer and compared it to the spectra obtained for the wild-type enzyme. For each measurement, 10 μM DNMT2 (wild type or variant) was dissolved in a buffer containing 10 mM Tris-HCl (pH 7.5) and 200 mM KCl. The spectra were recorded with a path length of 0.1 mm in the wavelength range between 190 and 250 nm with a step size of 0.1 nm and a bandwidth of 1 nm. For all spectra, 25 scans were performed and averaged. The baseline recorded for the buffer was subtracted from the protein spectra. All experiments were conducted at least twice.

Nitrocellulose Filter Binding Assay of $tRNA^{Asp}$ Binding. The $tRNA^{Asp}$ binding of wild-type and mutant DNMT2 was analyzed as described previously, using in vitro transcribed *D. melanogaster* $tRNA^{Asp}$, which was shown to be a competent substrate for the human DNMT2 enzyme.[13] The tRNA used in this study was radioactively labeled during the in vitro transcription step with [α-^{32}P]ATP, and the reaction buffer consisted of 100 mM Tris-HCl (pH 8), 100 mM NH_4OAc, 10 mM $MgCl_2$, 10 mM DTT, and 0.1 mM EDTA. All binding reactions were conducted at least twice. The binding constants for the variants were measured using the same batch of radioactively labeled tRNA that was used for the wild-type enzyme and under the same experimental conditions, such that these results could be directly compared. For each set of experiments with DNMT2 variants, the wild-type reaction was included as a positive control. Data were fit using the Excel solver module to an equation describing the equilibrium binding of tRNA to Dnmt2.

$$\mathrm{CPM} = \mathrm{BL} + F\left(\frac{c_{\mathrm{Dnmt2}}}{c_{\mathrm{Dnmt2}} + K_{\mathrm{d}}}\right)$$

where CPM is the radioactivity retained at the filter, BL is the baseline, and F is the signal intensity factor

Photo-Cross-Linking AdoMet Binding Experiments. Binding of AdoMet by DNMT2 was studied by photo-cross-linking of radioactively labeled [*methyl*-^{3}H]AdoMet (NEN) to the DNMT2 protein basically as described previously for Dnmt3a.[22] To this end, wild-type DNMT2 and its variants (4 μM) were incubated with radioactively labeled AdoMet (2 μM) in 10 μL of buffer [100 mM Tris-HCl (pH 8), 100 mM NH_4OAc, 10 mM $MgCl_2$, 1 mM DTT, and 0.1 mM EDTA] for 40 min on ice. Then, samples were irradiated using a UV cross-linker (Hoefer UVC 500, Amersham Biosciences) with UV (70000 mJ/cm^2, 254 nm) for 5 min on ice. The samples were then boiled in SDS loading buffer and electrophoresed on a SDS−15% (w/v) polyacrylamide gel. Protein loading was

dx.doi.org/10.1021/bi3002659 | *Biochemistry* 2012, 51, 4438−4444

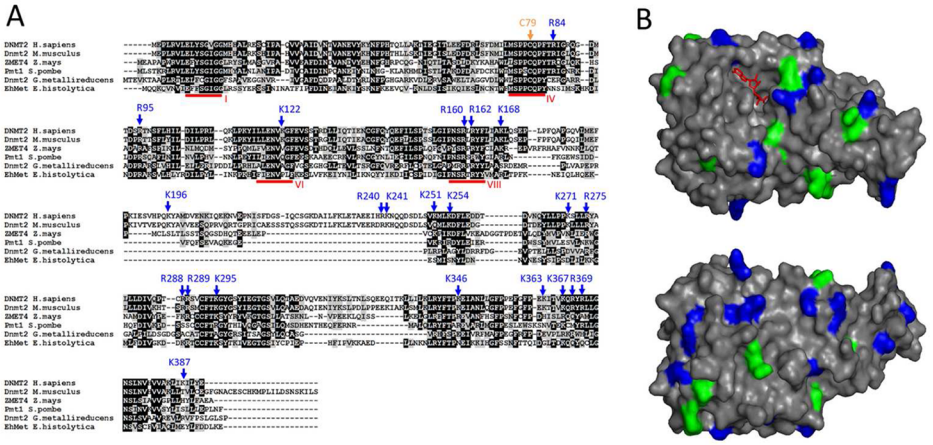

Figure 1. Multiple-sequence alignment and distribution of positively charged residues on the surface of human DNMT2. (A) Multiple-sequence alignment of the Dnmt2 enzymes generated using CLUSTALW and visualized in BIOEDIT. The characteristic catalytic motifs I, IV, VI, and VIII are indicated. (B) Crystal structure of human DNMT2 with the surface colored gray. Lysine and arginine residues are colored blue and green, respectively. The cofactor product SAH is shown as red sticks.

analyzed by Coomassie staining and AdoMet binding by autoradiography of the gels.

ANS Competition AdoMet Binding Experiments. AdoMet binding of DNMT2 was studied using a 1-anilinonaphthalene-8-sulfonic acid (CAS Registry No. 82-76-8) (ANS) competition assay basically as described previously for M.*Taq*I.[23] Fluorescence was measured in a Hitachi F-2500 spectrofluorimeter in 100 μL reaction volumes. Excitation was at 395 nm, and emission was recorded between 400 and 600 nm. Excitation and emission slits were set at 2.5 nm each. ANS fluorescence was determined as the average of the fluorescence between 480 and 520 nm. DNMT2 (1 μM) was incubated with ANS (50 μM) in buffer [100 mM Tris-HCl (pH 8), 100 mM NH_4OAc, 10 mM $MgCl_2$, 1 mM DTT, and 0.1 mM EDTA] for 5−10 min and fluorescence recorded. Binding of ANS to the AdoMet binding pocket of the methyltransferase led to a large increase in fluorescence. Then, AdoMet was added, and after incubation for 5−10 min, the fluorescence was measured. All binding reactions were conducted at least twice. Data were fit using the Excel solver module to an equation describing the equilibrium binding of AdoMet to DNMT2.

$$F = F_0\left(1 - \frac{c_{\text{AdoMet}}}{c_{\text{AdoMet}} + K_d}\right)$$

where F_0 is the fluorescence in the absence of AdoMet

In Vitro tRNA Methylation Assay. The methylation activity of wild-type human DNMT2 and its variants was studied with in vitro transcribed *D. melanogaster* $tRNA^{Asp}$ in a manner like that described previously.[24] Briefly, 2 μg (approximately 80 pmol) of $tRNA^{Asp}$ was incubated with 1 μM hDNMT2 protein in a 40 μL total reaction volume containing 100 mM Tris-HCl (pH 8), 100 mM NH_4OAc, 10 mM $MgCl_2$, 10 mM DTT, 0.1 mM EDTA, and 0.86 μM [*methyl*-^{3}H]AdoMet (NEN). We used relatively high enzyme concentrations to increase the dynamic range for the determination of the activity of mutants with weak activity. For each reaction, the tRNA was freshly refolded by incubation at 65 °C and slow cooling in the presence of Mg^{2+} ions. These improved conditions resulted in a significant increase in catalytic activity as compared to the results of previous experiments.[13] The reaction was started by the addition of the enzyme. At each of the chosen time points, a 2.5 μL aliquot was retrieved from the reaction mixture and added to a new tube containing 500 μL of 5% TCA to denature the enzyme and stop the reaction. Then, the samples were spotted on DE81 anion exchange paper disks (Whatman), washed with 5% TCA and 96% ethanol, and dried, and the incorporated tritium signal was quantified with a TriCarb 3170TR/SL (GE Healthcare) liquid scintillation counter. Linear regression analysis of the initial data points was used to extract the initial reaction rates, which correspond to the speed of the reaction in the first turnover. All RNA methylation assays were conducted in at least duplicate. For each set of activity experiments, the methylation reaction of wild-type DNMT2 was performed to allow direct comparison.

RESULTS

To select residues best suited to contribute to the tRNA binding pocket of human DNMT2, we have prepared a multiple-sequence alignment of Dnmt2 enzymes from various species and focused on positions with conserved basic residues (Figure 1A).[5] Next, we wanted to map the residues on the surface of DNMT2, therefore allowing us to determine putative tRNA binding pockets. In the published crystal structure of human DNMT2 [Protein Data Bank (PDB) entry 1G55],[3] the position of some loops was not determined because of their high mobility in the crystal. Because some of our selected residues are located within these loops, we have modeled them using Modeler. Although these loops are not resolved with atomic resolution in the final model, it still is valuable for the visualization of the general location of the studied residues. Positions of residues visible in the crystal structure were not changed significantly in the course of this modeling. Residues 172−250, which are not included in the structure, could not be modeled because of the large size of the part lacking. Using the partially modeled DNMT2 structure, we visualized all the positively charged residues on the surface of the protein (Figure 1B). To map the tRNA binding pocket, we have selected 20 residues (marked with arrows in Figure 1A) for mutagenesis, which are close to the catalytic center, as well as residues that are randomly distributed on different sides of the protein structure to roughly equally probe the protein surface.

dx.doi.org/10.1021/bi3002659 | *Biochemistry* 2012, 51, 4438−4444

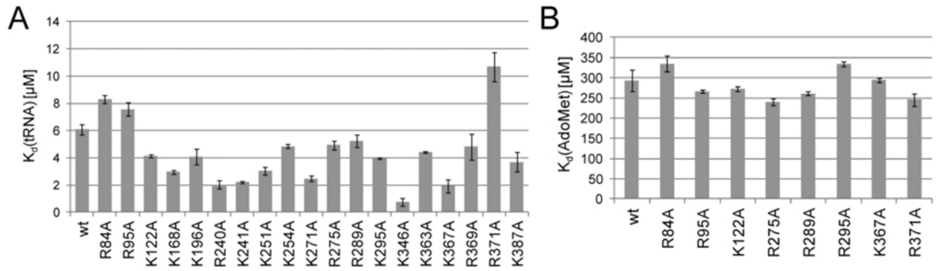

Figure 2. tRNA and AdoMet binding of wild-type Dnmt2 and its mutants. (A) Binding constants of $tRNA^{Asp}$ with wild-type DNMT2 and its mutants obtained by nitrocellulose filter binding assays (cf. Figure 2 of the Supporting Information). (B) Binding constants of AdoMet with wild-type DNMT2 and its mutants obtained by fluorescence ANS competition (cf. Figure 3B of the Supporting Information).

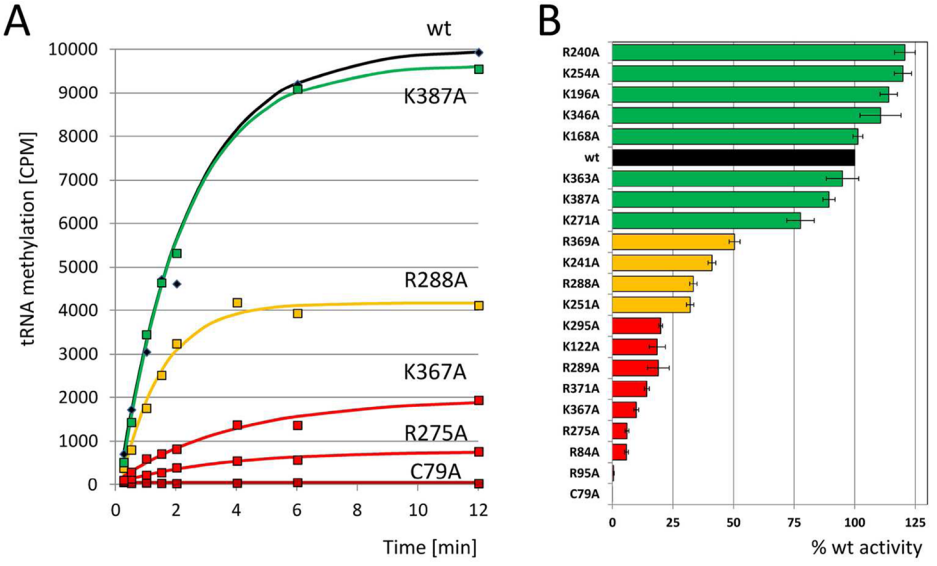

Figure 3. Catalytic activities of wild-type DNMT2 and its variants. (A) Exemplary reaction progress curves. The relative catalytic activities of mutant DNMT2 enzymes were extracted using linear regression analysis from the reaction progression curves. (B) Compilation of the results. The variants were categorized into three groups. Variants with wild-type-like activity (with maximally 2-fold reduced methylation activity) are colored green. Variants with 2−4-fold reduced methylation activity are colored orange, and variants with severely (>4-fold) reduced activity are colored red. The black bar represents 100% activity of the wild-type enzyme used as a reference. Error bars indicate the standard error of the mean. C79A is catalytically inactive[13] and served as a negative control. The single-turnover rate constant of wild-type DNMT2 ($17.4 \pm 0.7\ h^{-1}$) was determined by an exponential fit to the reaction progress curve.

Cloning, Site-Directed Mutagenesis, Protein Expression, and Purification. By site-directed mutagenesis, we have exchanged 20 lysine and arginine residues with alanine. The mutant genes were sequenced to confirm the introduction of the desired mutations and the absence of additional ones. All DNMT2 mutant proteins and the wild-type enzyme were expressed in *E. coli* cells and purified. The purified proteins were >90% pure (except for R84A, which was about 75% pure) as judged by SDS−PAGE and Coomassie staining (Figure 1 of the Supporting Information). The protein concentrations were determined by UV spectroscopy and validated by SDS−PAGE. All proteins were soluble and could be purified at concentrations in the range of 100−500 μM.

Far-UV Circular Dichroism Spectra. To confirm the correct folding of the mutant proteins, we have determined the far-UV circular dichroism (CD) spectra (which reflect the secondary structure composition of the protein) of all the DNMT2 variants. All CD spectra of DNMT2 variants were superimposable with the spectrum of the wild-type protein in the wavelength range of 195−240 nm, indicating that no large-scale folding deviations were caused by the introduced exchanges (Figure 1B of the Supporting Information).

RNA Binding of Wild-Type DNMT2 and Its Variants. We have investigated the $tRNA^{Asp}$ binding affinity of the wild-type DNMT2 protein and all its mutants using the nitrocellulose filter binding assay. In all experiments, constant amounts (0.4 nM) of the in vitro transcribed and radioactively labeled $tRNA^{Asp}$ were incubated with increasing amounts of wild-type DNMT2 or a variant and sucked through a nitrocellulose filter. The radioactivity retained on the membrane was read using a phosphorimager and quantified, and the resulting binding curves were fit by a bimolecular equilibrium binding model (Figure 2 of the Supporting Information) to determine the binding constants. As shown in Figure 2A, the weakest binding was observed with R371A, which had a residual binding constant that was 56% of that of the wild-type enzyme. R84 and R95 also exhibited slightly weakened binding. All other variants showed equilibrium tRNA binding that was the same as or better than that of the wild-type enzyme.

tRNA Methylation Activity of the Wild-Type and Mutant DNMT2 Enzymes. Once we confirmed the proper folding of the purified variants and determined their tRNA binding, we measured the $tRNA^{Asp}$ methylation activities of the

dx.doi.org/10.1021/bi3002659 | *Biochemistry* 2012, 51, 4438−4444

enzymes and compared them to the activity of wild-type DNMT2 (Figure 3). The methylation kinetics were determined using tritium-labeled AdoMet and in vitro transcribed and refolded $tRNA^{Asp}$. The obtained methylation data were fit by linear regression of the initial time points of the reaction to derive the initial rate of methylation under single-turnover conditions. Eight of the alanine exchange mutants had wild-type-like activity, with a <2-fold decrease in activity (K254A, R240A, K363A, K346A, K168A, K271A, K387A, and K196A), and four mutant proteins (R369A, R288A, K251A, and K241A) showed 2−4-fold decreases in activity (25−50% residual activity). However, eight mutants showed a large (>4-fold) decrease in catalytic activity (K122A, K295A, R289A, R371A, K367A, R275A, R84A, and R95A).

AdoMet Binding of the Mutants Showing Reduced Catalytic Activity. We observed decreases in catalytic activity with eight mutants (K122A, K295A, R289A, R371A, K367A, R275A, R84A, and R95A). Although none of these residues is directly involved in the AdoMet binding pocket, we wanted to assess AdoMet binding experimentally. Therefore, we determined the binding affinity of DNMT2 and its mutants with AdoMet by UV cross-linking using tritium-labeled AdoMet. As shown in Figure 3A of the Supporting Information, AdoMet binding showed only small deviations between wild-type DNMT2 and its variants. Because it is difficult to derive a quantitative binding constant with the results of the cross-linking assay, we also employed a fluorescence assay in which AdoMet competes with binding of ANS to the AdoMet binding pocket.[23] Binding of ANS to the enzyme leads to a large increase in fluorescence. Afterward, AdoMet was added, which competes with the ANS for DNMT2 binding and leads to a decrease in fluorescence (Figure 3 of the Supporting Information). We determined a K_d of 290 μM (±10 μM, standard error) for binding of AdoMet to wild-type DNMT2. Binding to all mutants was identical within ±20%, indicating that the mutations do not interfere with AdoMet binding (Figure 2B). Because none of the residues exchanged in these mutants is involved in chemical steps of catalysis, we conclude that they have a role in the interaction of Dnmt2 with the tRNA during catalysis.

DISCUSSION

Mapping of the tRNA Binding Site of DNMT2. To map the $tRNA^{Asp}$ interaction of human DNMT2, we mutated 20 conserved basic residues to alanine, purified the mutant proteins, and investigated their catalytic activity. Eight variants displayed strongly decreased activity (R95A, R84A, R275A, K367A, R371A, R289A, K295A, and K122A). The weakest methylation activity (<1% of wild-type activity) in this study was observed for the R95A variant. The R95 residue is strongly conserved in the alignment of DNMT2 enzymes (Figure 1A) and is located in the nearest neighborhood of the cofactor. The DNMT2 R84A enzyme variant was the second weakest active DNMT2 protein variant and retained only approximately 5% of the wild-type activity. The strongly conserved R84 residue is localized in catalytic motif IV, in the proximity of the catalytic cysteine in the putative catalytic pocket of the enzyme. The other residues that were important for methylation activity (R275, K367, R371, R289, K295, and K122 in order of increasing residual activity) all are localized on one side of the protein (Figure 4) in a shallow surface groove present on the "front" side of the DNMT2 protein. It extends from the cofactor binding site and includes the residues forming the

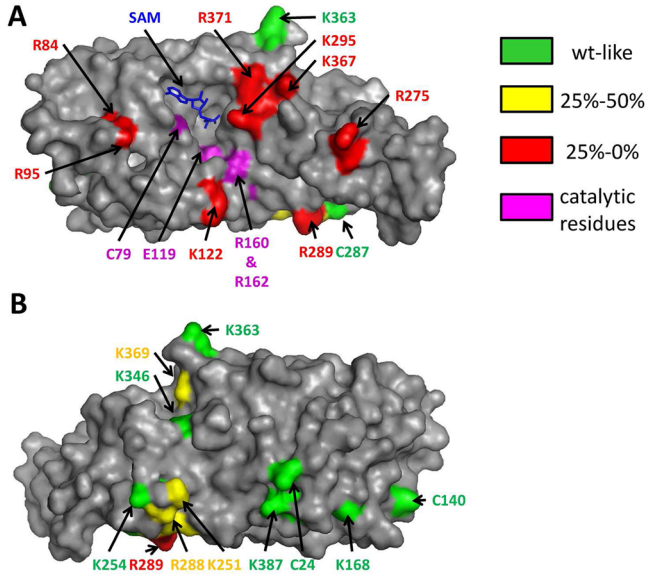

Figure 4. Different views of DNMT2 in surface representation. The residues subjected to mutagenesis were colored according to their residual activity. The cofactor product *S*-adenosyl-L-homocysteine is colored blue. Residues that strongly interfere with catalysis (colored red here) cluster on the "front" face of the enzyme and surround a cleft that also contains the AdoMet binding pocket and the catalytic residues. To provide a complete picture, C24, C140, and C287, the alanine exchange of which was previously shown not to reduce activity,[13] are also included. Panel B represents a view of the "back side" of the enzyme after a 180° rotation of the view shown in panel A about the vertical axis.

catalytic pocket (C79, R160, and R162).[13] Strikingly, the residues important for the activity identified here clearly cluster along this groove (Figures 4 and 5A), which strongly suggests that it represents the binding site for the tRNA. In contrast, the residues that have little or no influence on the methylation activity are distributed on the other side of the protein, indicating that the back side of the surface is not taking part in the tRNA interaction.

DNMT2 Induces a Conformational Change of the DNMT2-tRNA Complex. DNMT2 induces a conformational change in the tRNA. As described above, R95, R84, R275, K367, R371, R289, K122, and K295 (in order of increasing residual activity) showed a large decrease in tRNA methylation activity. With most of these variants, much smaller differences in the tRNA binding constants were observed, but they are not sufficient to explain the large differences in catalytic activities. Specifically, the level of tRNA binding of R95A and R84A was 80 and 73% of the level of wild-type binding, respectively, although catalytic activities are smaller than 1 and 5%, respectively. R275, K367, R289, K295, and K122 all showed tRNA binding better than that of the wild type. For only one variant (R371A) was the decrease in catalytic activity similar to the decrease in the level of tRNA binding.

The general function of an enzyme includes binding of the substrate in a ground state complex, which then changes into the transition state of the catalyzed reaction. The transition state is stabilized by the enzyme, which is one principle of enzymatic catalysis. Mutations disrupting contacts of the enzyme and substrate in the ground state and/or transition state are expected to lower the substrate binding and/or catalytic efficiency, respectively. The results obtained with the

dx.doi.org/10.1021/bi3002659 | *Biochemistry* 2012, 51, 4438−4444

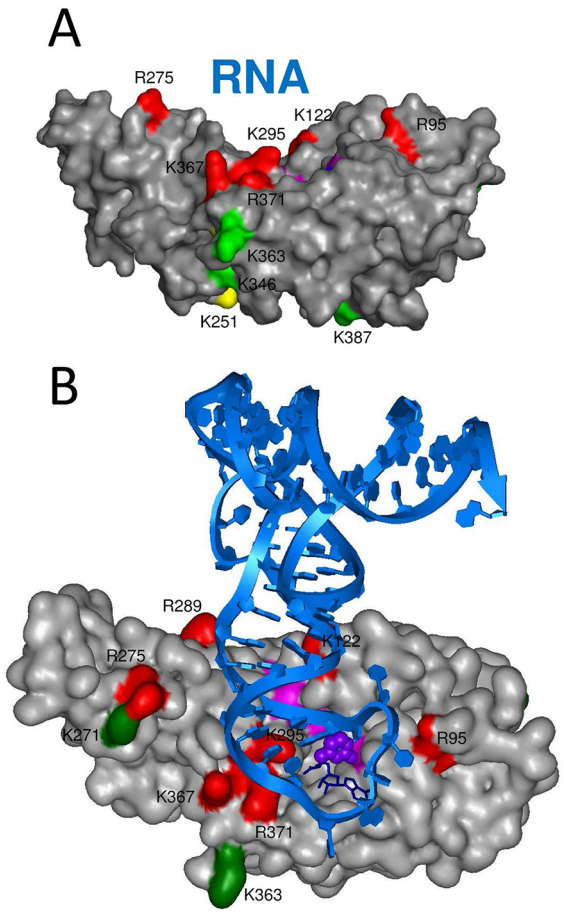

Figure 5. tRNA binding groove of DNMT2 colored as described in the legend of Figure 4. (A) Visualization of the surface cleft containing critical and active site residues that is the putative tRNA binding site. (B) Model with manually placed $tRNA^{Asp}$ such that the target base could approach its binding pocket. The tRNA is colored blue, with the target nucleotide colored purple and shown in space-filling representation.

R371A variant suggest a role of this residue in ground state and transition state tRNA binding. The effects of the other mutations observed here suggest that the corresponding residues participate in transition state interaction but not or not so much in ground state binding. It is particularly striking that many variants showed decreased catalytic efficiencies, but even stronger tRNA binding. This result suggests that the enzyme induces an energetically unfavorable conformational change in the tRNA when it approaches the transition state. If a mutation disrupts this step, catalytic activity declines, but the ground state tRNA binding improves, because the unfavorable change into the transition state conformation is avoided.

Manual Placement of $tRNA^{Asp}$ into the DNMT2 Structure. It turned out that eight of the variants prepared here showed a large decrease in activity, and all of them cluster on one side of the surface of DNMT2 surrounding a surface cleft roughly fit in size to the anticodon stem–loop part of the tRNA (Figures 4 and 5A). To obtain an impression of the size of the identified tRNA binding cleft and the tRNA, we took the $tRNA^{Asp}$ structure from the complex of aspartyl-tRNA synthetase with $tRNA^{Asp}$ (PDB entry 1ASY)[25] and manually placed it into the structure of DNMT2 such that the target cytosine in the anticodon loop could reach the catalytic cysteine residue and the cofactor (Figure 5B). In this step, the potential rotation of the target base about the phosphodiester backbone was considered. Given the size and shape of the tRNA binding pocket, the modeling suggests that the main contacts of DNMT2 should be with the anticodon loop and stem of the tRNA. Our attempts to place the tRNA in the binding pocket of the enzyme also indicated a second interesting point. The active site of the enzyme is located on the right side of the RNA binding cleft in the orientation of the enzyme shown in Figure 5B. Because of this, the positioning of the target base an appropriate distance from the catalytic residues was only possible if the acceptor stem of the L-shaped tRNA pointed away from the enzyme. This result suggests that the CCA end and acceptor stem are not contacted by Dnmt2, which is in agreement with the observation that no strong effects were observed after mutation of residues on the "side" or "back" face of the enzyme.

CONCLUSIONS

We successfully mapped the tRNA binding pocket of DNMT2. The observed changes in catalytic activity and tRNA binding suggest that the enzyme-RNA complex undergoes a conformational changes while approaching the transition state of the methyl group transfer reaction. Placement of $tRNA^{Asp}$ into the structure suggests that DNMT2 mainly interacts with the anticodon stem and loop.

ASSOCIATED CONTENT

Supporting Information

Purified His_6-DNMT2 variants (Figure 1), nitrocellulose filter binding assays for studying the binding of $tRNA^{Asp}$ by wild-type DNMT2 and its mutants (Figure 2). and AdoMet binding assay with wild-type DNMT2 and its mutants with reduced catalytic efficiency (Figure 3). This material is available free of charge via the Internet at http://pubs.acs.org.

AUTHOR INFORMATION

Corresponding Author

*Institute of Biochemistry, Faculty of Chemistry, Stuttgart University, Pfaffenwaldring 55, D-70569 Stuttgart, Germany. Phone: +49 711 685 64390. Fax: +49 711 685 64392. E-mail: albert.jeltsch@ibc.uni-stuttgart.de.

Author Contributions

T.P.J. and R.S. contributed equally to this work.

Funding

This work has been supported by the DFG FOR 1082 (Je 252/8).

Notes

The authors declare no competing financial interest.

ACKNOWLEDGMENTS

We acknowledge experimental support provided by Nicolae Solcan, Ranjan Mishra, and Agnieszka Bruzda.

ABBREVIATIONS

ANS, 1-anilinonaphthalene-8-sulfonic acid; AdoMet, *S*-adenosyl-L-methionine; CD, circular dichroism.

REFERENCES

(1) Van den Wyngaert, I., Sprengel, J., Kass, S. U., and Luyten, W. H. (1998) Cloning and analysis of a novel human putative DNA methyltransferase. *FEBS Lett. 426*, 283–289.

(2) Yoder, J. A., and Bestor, T. H. (1998) A candidate mammalian DNA methyltransferase related to pmt1p of fission yeast. *Hum. Mol. Genet. 7*, 279−284.
(3) Dong, A., Yoder, J. A., Zhang, X., Zhou, L., Bestor, T. H., and Cheng, X. (2001) Structure of human DNMT2, an enigmatic DNA methyltransferase homolog that displays denaturant-resistant binding to DNA. *Nucleic Acids Res. 29*, 439−448.
(4) Jeltsch, A., Nellen, W., and Lyko, F. (2006) Two substrates are better than one: Dual specificities for Dnmt2 methyltransferases. *Trends Biochem. Sci. 31*, 306−308.
(5) Jurkowski, T. P., and Jeltsch, A. (2011) On the evolutionary origin of eukaryotic DNA methyltransferases and dnmt2. *PLoS One 6*, e28104.
(6) Okano, M., Xie, S., and Li, E. (1998) Dnmt2 is not required for de novo and maintenance methylation of viral DNA in embryonic stem cells. *Nucleic Acids Res. 26*, 2536−2540.
(7) Hermann, A., Schmitt, S., and Jeltsch, A. (2003) The human Dnmt2 has residual DNA-(cytosine-C5) methyltransferase activity. *J. Biol. Chem. 278*, 31717−31721.
(8) Fisher, O., Siman-Tov, R., and Ankri, S. (2004) Characterization of cytosine methylated regions and 5-cytosine DNA methyltransferase (Ehmeth) in the protozoan parasite *Entamoeba histolytica*. *Nucleic Acids Res. 32*, 287−297.
(9) Kuhlmann, M., Borisova, B. E., Kaller, M., Larsson, P., Stach, D., Na, J. B., Eichinger, L., Lyko, F., Ambros, V., Soderbom, F., Hammann, C., and Nellen, W. (2005) Silencing of retrotransposons in *Dictyostelium* by DNA methylation and RNAi. *Nucleic Acids Res. 33*, 6405−6417.
(10) Goll, M. G., Kirpekar, F., Maggert, K. A., Yoder, J. A., Hsieh, C. L., Zhang, X., Golic, K. G., Jacobsen, S. E., and Bestor, T. H. (2006) Methylation of tRNAAsp by the DNA methyltransferase homolog Dnmt2. *Science 311*, 395−398.
(11) Phalke, S., Nickel, O., Walluscheck, D., Hortig, F., Onorati, M. C., and Reuter, G. (2009) Retrotransposon silencing and telomere integrity in somatic cells of *Drosophila* depends on the cytosine-5 methyltransferase DNMT2. *Nat. Genet. 41*, 696−702.
(12) Schaefer, M., and Lyko, F. (2010) Lack of evidence for DNA methylation of Invader4 retroelements in *Drosophila* and implications for Dnmt2-mediated epigenetic regulation. *Nat. Genet. 42*, 920−921.
(13) Jurkowski, T. P., Meusburger, M., Phalke, S., Helm, M., Nellen, W., Reuter, G., and Jeltsch, A. (2008) Human DNMT2 methylates tRNA(Asp) molecules using a DNA methyltransferase-like catalytic mechanism. *RNA 14*, 1663−1670.
(14) Schaefer, M., Pollex, T., Hanna, K., and Lyko, F. (2009) RNA cytosine methylation analysis by bisulfite sequencing. *Nucleic Acids Res. 37*, e12.
(15) Schaefer, M., Pollex, T., Hanna, K., Tuorto, F., Meusburger, M., Helm, M., and Lyko, F. (2010) RNA methylation by Dnmt2 protects transfer RNAs against stress-induced cleavage. *Genes Dev. 24*, 1590−1595.
(16) Tovy, A., Siman Tov, R., Gaentzsch, R., Helm, M., and Ankri, S. (2010) A new nuclear function of the *Entamoeba histolytica* glycolytic enzyme enolase: the metabolic regulation of cytosine-5 methyltransferase 2 (Dnmt2) activity. *PLoS Pathog. 6*, e1000775.
(17) Cheng, X. (1995) Structure and function of DNA methyltransferases. *Annu. Rev. Biophys. Biomol. Struct. 24*, 293−318.
(18) Jeltsch, A. (2002) Beyond Watson and Crick: DNA methylation and molecular enzymology of DNA methyltransferases. *ChemBioChem 3*, 274−293.
(19) Jeltsch, A., and Lanio, T. (2002) Site-directed mutagenesis by polymerase chain reaction. *Methods Mol. Biol. 182*, 85−94.
(20) Sali, A., Potterton, L., Yuan, F., van Vlijmen, H., and Karplus, M. (1995) Evaluation of comparative protein modeling by MODELLER. *Proteins 23*, 318−326.
(21) Guex, N., and Peitsch, M. C. (1997) SWISS-MODEL and the Swiss-PdbViewer: An environment for comparative protein modeling. *Electrophoresis 18*, 2714−2723.
(22) Gowher, H., Loutchanwoot, P., Vorobjeva, O., Handa, V., Jurkowska, R. Z., Jurkowski, T. P., and Jeltsch, A. (2006) Mutational analysis of the catalytic domain of the murine Dnmt3a DNA-(cytosine C5)-methyltransferase. *J. Mol. Biol. 357*, 928−941.
(23) Schluckebier, G., Kozak, M., Bleimling, N., Weinhold, E., and Saenger, W. (1997) Differential binding of S-adenosylmethionine S-adenosylhomocysteine and Sinefungin to the adenine-specific DNA methyltransferase M.TaqI. *J. Mol. Biol. 265*, 56−67.
(24) Tovy, A., Hofmann, B., Helm, M., and Ankri, S. (2010) In vitro tRNA Methylation Assay with the *Entamoeba histolytica* DNA and tRNA Methyltransferase Dnmt2 (Ehmeth) Enzyme. *J. Visualized Exp.*, e2390.
(25) Ruff, M., Krishnaswamy, S., Boeglin, M., Poterszman, A., Mitschler, A., Podjarny, A., Rees, B., Thierry, J. C., and Moras, D. (1991) Class II aminoacyl transfer RNA synthetases: Crystal structure of yeast aspartyl-tRNA synthetase complexed with tRNA(Asp). *Science 252*, 1682−1689.